JOURNAL OF GUIDANCE, CONTROL, AND DYNAMICS
Vol. 15, No. 4, July-August 1992

# Wideband Control of Gyro/Accelerometer Multisensors in a Strapdown Guidance System

Pierre Constancis
*SAGEM, 95523 Cergy-Pontoise, France*
and
Michel Sorine
*Institut National de Recherche en Informatique et Automatique, 78153 Le Chesnay, France*

**This paper describes an inertial measurement unit based on three dry tuned gyroscopes, two of which are unbalanced. This configuration, without the three usual accelerometers, leads to savings in space, weight, and cost that are necessary in guidance systems for agile missiles. Design objectives are wideband estimation of angular rate and linear acceleration applied to the inertial measurement unit together with high stiffness of caging loops. The contribution of this paper is to show how to address the coupled high-frequency dynamics of the six measurement outputs of the system, by applying the so-called linear quadratic Gaussian technique. First the linearized model of the rotor motion of each dry-tuned gyroscope is derived from a mechanical analysis. Then the design of the controller/estimator is described. Performances are illustrated with test data.**

## Nomenclature

$[a]$ = $3 \times 3$ diagonal matrix where $a_i$ are real numbers $\begin{bmatrix} a_1 & 0 & 0 \\ 0 & a_2 & 0 \\ 0 & 0 & a_3 \end{bmatrix}$

$D_i$ = rotor windage damping coefficient for gyroscope $i$

$F$ = difference between the absolute linear acceleration of the inertial measurement unit and the gravity acceleration in the $X, Y, Z$ frame

$f = \begin{pmatrix} f_1 \\ f_2 \\ f_3 \end{pmatrix}$

$f_i$ = projection of $F$ on the input plane $x_i$, $y_i$ of gyroscope $i$ ($i = 1,2,3$)

$I_i$ = mean radial moment of the rotor of gyroscope $i$

$I_n$ = $n$-dimensional identity matrix

$I_{zi}$ = principal moment of inertia of the rotor about the $z_i$ axis

$J$ = in quadrature matrix used in gyroscope equations, $= \begin{bmatrix} 0 & -1 \\ 1 & 0 \end{bmatrix}$

$K_{qi}$ = rotor-to-case lift torque coefficient for gyroscope $i$

$K_{\varphi i}$ = residual stiffness of flexures for gyroscope $i$

$N_i$ = angular velocity of the motor shaft relative to the casing, about $z_i$ axis

$P_i$ = rotor pendulosity along spin axis for gyroscope $i$

$X, Y, Z$ = axes of the reference frame of the inertial measurement unit

$x_i, y_i, z_i$ = axes of the reference frame of gyroscope $i$ ($i = 1,2,3$), $x_i$ and $y_i$ being the two input axes, and $z_i$ the spin axis

$\beta = \begin{pmatrix} \beta_1 \\ \beta_2 \\ \beta_3 \end{pmatrix}$

$\beta_i$ = angular position of the rotor relative to the case, about $x_i$ and $y_i$ axes for gyroscope $i$ ($i = 1,2,3$)

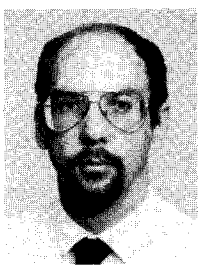

**Pierre Constancis graduated from Ecole Centrale de Lyon, France, in 1981. Since then he has been engaged in the development and design of digital controllers at SAGEM, as a Research Engineer. He received his doctoral degree in March 1990 from the University of Paris IX. His present research interests are robust and adaptive control and mobile robot guidance. He is a member of the AIAA.**

**Michel Sorine is Research Director at the Institute National de Recherche en Informatique et Automatique (INRIA). He also teaches computer control of industrial processes at the University of Paris IX. His current research interests include automatic control of lumped and distributed-parameter systems, signal processing, and real-time programming.**

Received June 15, 1989; presented as Paper 89-3441 at the AIAA Guidance, Navigation, and Control Conference, Boston, MA, Aug. 14-16, 1989; revision received Sept. 12, 1990; accepted for publication April 18, 1991. 

$\nu_i$ = nutation frequency for gyroscope $i$, $I_{zi}N_i/I_i$

$\sigma_{max}(A)$ = maximum singular value of the matrix $A$, which is also the spectral norm of $A$

$\Omega$ = absolute angular rate of the inertial measurement unit, in the $X,Y,Z$ frame

$$\tilde{\Omega} = \begin{pmatrix} \Omega \\ F \end{pmatrix}$$

$$\omega = \begin{pmatrix} \omega_1 \\ \omega_2 \\ \omega_3 \end{pmatrix}$$

$$\omega_c = \begin{pmatrix} \omega_{c1} \\ \omega_{c2} \\ \omega_{c3} \end{pmatrix}$$

$\omega_{ci}$ = angular velocity such that, for gyroscope $i$, the projection on the input plane $x_i$, $y_i$ of the torque applied to the rotor is $-I_{zi}N_iJ\omega_{ci}$ $(i = 1,2,3)$

$\omega_i$ = projection of $\Omega$ on the input plane $x_i$, $y_i$ of gyroscope $i$ $(i = 1,2,3)$

$\otimes$ = Kronecker product of matrices. Let $A$ be $p \times q$ and $B$ be $r \times s$: $A \otimes B$ is $pr \times qs$ and has $p \times q$ partitions. The $i$-$j$ partition is $A_{ij} \cdot B$

## Introduction

A FAMILY of strapdown inertial measurement units (IMUs) for angular rate and acceleration measurements has been developed. It answers the needs for miniature wideband attitude and navigation systems for missile guidance. For reasons of size, weight, and cost, the only sensors used in these systems are three dry tuned gyroscopes (DTGs), two of which are unbalanced (UDTG), instead of three accelerometers and two balanced DTGs.

Design objectives are wideband estimation of angular rate and linear acceleration applied to the IMU together with high stiffness of caging loops. The contribution of this paper is to show how to address the coupled high-frequency dynamics of the six measurement outputs of the system by applying the so-called linear quadratic Gaussian (LQG) technique.

Because of their small size and low price, high-speed microprocessors have made it possible to choose this digital technique. Earlier work[1] on the design of a digital servo-control loop for a gyro led to problems of robustness due to parameter variations. More recently, Riberio[2] proposed a LQG control for a similar gyroscope, using a simplified mode. Both studies assumed that gyro angular rate is proportional to controller torque, which is not the case during fast variations of angular rate. The LQG control described in this section is based on a more sophisticated model inspired by Craig[3] that takes into account the multivariable nature and high-frequency dynamics (from dc to nutation) of each UDTG. In contrast to previous studies, our estimator is based on a stochastic model of angular rate and linear acceleration instead of being taken proportional to controller torques.[2] Thus, the bandwidth of the estimator is greater than the bandwidth of the closed loop.

The organization of the paper is the following. The UDTG is first described, then the principle of acceleration and angular rate measurement is presented and followed by a detailed description of the LQG estimation and control design. Finally, performances are illustrated with test data and discussed.

## Model of the Unbalanced Dry Tuned Gyroscope

Each gyroscope used in the IMU is similar to the one presented in Fig. 1. It has a diameter of about 3 cm. The main components are as follows:

1) The drive motor, a two-phase, synchronous hysteresis type, spins the rotor, at a high angular velocity $N(\pm 250$ revolutions/s).

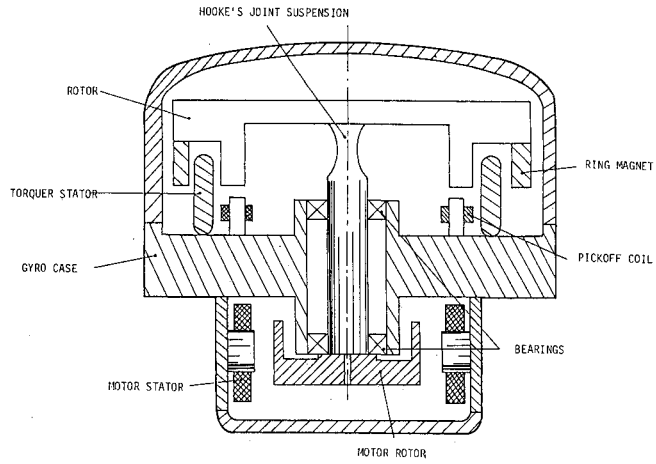


**Fig. 1 Cross section of a dry-tuned gyro.**

2) The suspension is a Hooke's joint containing one gimbal connected to the rotor, on one side, and the motor shaft by two orthogonal elastic hinges, on the other side. The rotor is then free to rotate about these two axes. The spring rate of the flexure is dynamically tuned to nearly zero. Perfect adjustment is not necessary because the model takes into account the residual stiffness.

3) The rotor c.m. is chosen distinct from the center of torsional support (unbalanced gyro). This rotor axial pendulosity is responsible for its sensitivity to linear acceleration inputs.

4) The inductive pickoffs measure the rotor angular position $\beta_i$ about the $x_iy_i$ input axes.

5) Two magnetic torquers, oriented along these gyro input axes, exert a moment on the rotor interpreted as an angular rate $\omega_{ci}(t)$. In a forced-balance sensor like the present one, $\omega_{ci}$ is chosen so that the rotor follows the case motion. $\beta_i$ is the regulation error. These torquers are powerful enough for strapdown applications.

6) Because of the gas contained inside the case, an aerodynamic moment as well as a damping moment act on the rotor.

The method used by Craig[3,4] for the case of UDTG leads to the following equation of motion[5]:

$$\ddot{\beta}_i + [(D_i/I_i)I_2 - \nu_i J]\dot{\beta}_i + \nu_i(K_{\varphi i}I_2 - K_{qi}J)\beta_i = -\dot{\omega}_i + \nu_i J(\omega_i - \omega_{ci}) - (P_i/I_i)Jf_i \quad (1)$$

## Principle of Angular Rate and Acceleration Measurements

Each $K_{\varphi i}$ is made small by tuning the UDTG. $K_{qi}$ and $D_i$ are also made small by choosing a light gas. So $\nu_i$ is the main coefficient of Eq. (1).

First consider the classical DTG ($P_i = 0$) and suppose that $N_i$ (and so $\nu_i$) is much greater than the bandwidth of $\omega_i$. In this case, Eq. (1) can be simplified into

$$\dot{\beta}_i = \omega_{ci} - \omega_i \quad (2)$$

The principle of the forced-balance sensor consists in zeroing the output $\beta_i$ with an appropriate control $\omega_{ci}$ and so it appears that a possible estimation of $\omega_i$ is given by

$$\hat{\omega}_i = \omega_{ci} \quad (3)$$

which is identical to previously used estimators.[1,3]

Remaining in the case where $P_i = 0$, let us suppose that the bandwidth of $\omega_i$ is comparable to $N_i$. The estimation given by Eq. (3) is no longer sufficient because $\beta_i$ is no longer negligi-

ble, as the nearly undamped nutation frequency is being excited. In this case it is possible, as we will show later, to use the more complete model of Eq. (1) to improve the estimation of Eq. (3).

Now let us see why the principle of forced-balance sensor is still valid for a system of three UDTGs.

Equation (1) for $i = 1,2,3$ can be rewritten into a higher dimensional matrix equation:

$$\ddot{\beta} + ([D/I] \otimes I_2 - [\nu] \otimes J)\dot{\beta} + ([\nu] \otimes I_2) \cdot ([K_\varphi] \otimes I_2 - [K_q] \otimes J)\beta = -\dot{\omega} + ([\nu] \otimes J) \cdot (\omega - \omega_c) - ([P/I] \otimes J)f \tag{4}$$

The true inputs of this model are $\omega_c$ and $\tilde{\Omega}$, which lead to expressing $\omega, f$ as functions of $\tilde{\Omega}$. Figure 2 shows the relations between the reference frame of each gyroscope and the reference frame of the system:

$$\begin{cases} x_1 = X \\ y_1 = Y \\ x_2 = Z \\ y_1 = X \\ x_3 = Y \\ y_3 = Z \end{cases} \tag{5}$$

Relations between $\omega, f$ and $\tilde{\Omega}$ are deduced:

$$\omega = \left[\begin{pmatrix} 1 & 0 \\ 1 & 0 \end{pmatrix} \otimes I_3\right]\tilde{\Omega}, \qquad f = \left[\begin{pmatrix} 0 & 1 \\ 0 & 1 \end{pmatrix} \otimes I_3\right]\tilde{\Omega} \tag{6}$$

The right member of Eq. (4) can now be rewritten:

$$E = -\dot{\omega} + ([\nu] \otimes J)(\omega - \omega_c) - ([P/I] \otimes J)f$$

$$= -\dot{\omega} + ([\nu] \otimes J)(\omega - \omega_c) + ([\nu] \cdot [\rho]) \otimes (J \cdot I_2)f$$

where

$$\rho_i = -(P_i/I_{zi}N_i) \tag{7}$$

The mixed rule product of Kronecker algebra[9]

$$\begin{cases} (A \otimes B) \cdot (C \otimes D) = (A \cdot C) \otimes (B \cdot D) \\ \text{as soon as the usual products } A \cdot C \text{ and} \\ B \cdot D \text{ are defined} \end{cases} \tag{8}$$

leads to

$$E = -\dot{\omega} + ([\nu] \otimes J)(\omega - \omega_c) + ([\nu] \otimes J) \cdot ([\rho] \otimes I_2) \cdot f$$

$$= -\dot{\omega} + ([\nu] \otimes J) \cdot \{\omega + ([\rho] \otimes I_2)f - \omega_c\}$$

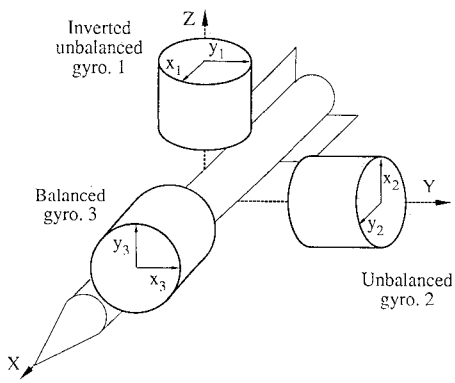


**Fig. 2 Definition of coordinate reference frames.**

and finally

$$E = -\left[\begin{pmatrix} 1 & 0 \\ 1 & 0 \end{pmatrix} \otimes I_3\right]\dot{\tilde{\Omega}} + ([\nu] \otimes J)(U\tilde{\Omega} - \omega_c) \tag{9}$$

with

$$U = \begin{pmatrix} 1 & 0 \\ 1 & 0 \end{pmatrix} \otimes I_3 + ([\rho] \otimes I_2)\left[\begin{pmatrix} 0 & 1 \\ 0 & 1 \end{pmatrix} \otimes I_3\right] \tag{10}$$

As soon as $U$ is invertible, the comparison of Eq. (4) and Eq. (9) to Eq. (1) shows that the principle of forced-balance sensors can be applied, a first estimation of $\tilde{\Omega}$ being given by

$$\hat{\tilde{\Omega}} = U^{-1}\omega_c \tag{11}$$

A key step is enforcing invertibility of $U$ by choosing $[\rho]$. Splitting $[\rho] \otimes I_2$ into four $3 \times 3$ blocks leads to

$$[\rho] \otimes I_2 = \begin{pmatrix} R_1 & 0 \\ 0 & R_2 \end{pmatrix}$$

with

$$R_1 = \begin{pmatrix} \rho_1 & 0 & 0 \\ 0 & \rho_1 & 0 \\ 0 & 0 & \rho_2 \end{pmatrix}, \qquad R_2 = \begin{pmatrix} \rho_2 & 0 & 0 \\ 0 & \rho_3 & 0 \\ 0 & 0 & \rho_3 \end{pmatrix} \tag{12}$$

so that

$$U = \begin{pmatrix} I_3 & R_1 \\ I_3 & R_2 \end{pmatrix} = \begin{pmatrix} I_3 & 0 \\ I_3 & -I_3 \end{pmatrix} \cdot \begin{pmatrix} I_3 & R_1 \\ 0 & R_1 - R_2 \end{pmatrix} \tag{13}$$

$U$ is invertible as soon as $R_1 - R_2$ is invertible; that is to say, as soon as $\rho_1 \neq \rho_j \ \forall i \neq j$, $i,j = 1,2,3$.

In that case

$$U^{-1} = \begin{bmatrix} I_3 - R_1(R_1 - R_2)^{-1} & R_1(R_1 - R_2)^{-1} \\ (R_1 - R_2)^{-1} & -(R_1 - R_2)^{-1} \end{bmatrix} \tag{14}$$

In the present realization, gyro 3 is chosen balanced and gyro 2 is inverted relative to gyro 1 ($N_2 = -N_1$):

$$\rho_3 = 0, \qquad \rho_2 = -\rho_1 \neq 0 \tag{15}$$

## LQG Estimation and Control Design for the IMU

To improve this estimator (11), the proposed method takes into account the high-frequency dynamics modeled by Eq. (4).

An estimation and a feedback control are requested:

$$\begin{cases} \hat{\tilde{\Omega}}(K) = E\{\tilde{\Omega}(k) | y(k-1), y(k-2), \ldots\} \\ \omega_c(k) = \phi[y(k-1), y(k-2), \ldots] \end{cases} \tag{16}$$

Sampled noisy measurements $y(k-1)$, $y(k-2)$, ... are assumed to be known at time $k$:

$$y(k) = \beta(k) + w(k) \tag{17}$$

where $w$ is a six-dimensional discrete-time Gaussian white noise, with covariance $R$.

The control $\omega_c$ is chosen to minimize the following quadratic loss function:

$$J\omega_c = \lim_{n \to \infty} \frac{1}{n} E\left\{\sum_{k=0}^{n} |\beta(k)|^2 + q^2|\omega_c(k) - U\tilde{\Omega}(k)|^2\right\} \tag{18}$$

As usual, the control variable is penalized in order to limit the feedback gains. Here, this penalization is chosen as the square of the distance between the control and the static forced-balance control [cf. Eq. (11)].

To solve this estimation and control problem, an augmented state is introduced:

$$x = \begin{pmatrix} x_1 \\ x_2 \\ x_3 \\ \tilde{\Omega} \end{pmatrix} \quad \text{vector of 18 real variables} \tag{19}$$

with

$$x_i = \begin{pmatrix} \beta_i \\ . \\ \beta_i \end{pmatrix} \quad \text{vector of 18 real variables}$$

To eliminate static estimation errors, the stochastic model of $\tilde{\Omega}$ is chosen to be a random drift:

$$\dot{\tilde{\Omega}}(t) = \nu_\Omega(t) \tag{20}$$

where $\nu_\Omega$ is a six-dimensional Gaussian white noise, independent of $w$, with covariance

$$\begin{pmatrix} \sigma_\Omega^2 & 0 \\ 0 & \sigma_F^2 \end{pmatrix} \otimes I_3$$

Equations (4), (9), and (20) are then discretized, leading to the state equations:

$$x(k+1) = Fx(k) + G\omega_c(k) + \nu(k) \tag{21}$$

where $\nu$ is a Gaussian white noise with covariance $Q$.

The observation is

$$y(k) = Hx(k) + w(k) \tag{22}$$

with $H = (1,0,0) \otimes I_6$.

The solution of the estimation problem for $x$ and so, in particular for $\tilde{\Omega}$, is given by

$$\begin{cases} \hat{x}(k+1) = F\hat{x}(k) + G\omega_c(k) + K[y(k) - H\hat{x}(k)] \\ E[x(k) \mid y(k-1), y(k-2), \ldots] = \hat{x}(k) \end{cases} \tag{23}$$

where $K$ is the steady-state Kalman filter gain computed off line via the solution of a Riccati equation associated with the observable pair $(F,H)$:

$$P = FPF^t - FPH^t(HPH^t + R)^{-1}HPF^t + Q \tag{24}$$

$$K = FPH^t(HPH^t + R)^{-1} \tag{25}$$

Applying the so-called separation principle of the LQG theory,[6] the solution of the control problem can be computed assuming the knowledge of $x$ and without noise. But $\tilde{\Omega}$ is neither controllable nor observable through the quadratic cost function $J$. A minimal realization is obtained by changing the control variable $\omega_c$ into $u$:

$$u = \omega_c - U\tilde{\Omega} \tag{26}$$

and the state feedback of the whole system can be split into three parts (one per gyro), so that the implementation can be simplified. Let

$$u = \begin{pmatrix} u_1 \\ u_2 \\ u_3 \end{pmatrix} \tag{27}$$

so that Eqs. (21) and (22) are reduced to

$$\begin{cases} x_i(k+1) = F_i x_i(k) + G_i u_i(k) \\ \beta_i(k) = H_i x_i(k) \end{cases} \tag{28}$$

for $i = 1,2,3$.

The quadratic loss function of Eq. (18) is then

$$J(u) = J_1(u_1) + J_2(u_2) + J_3(u_3) \tag{29}$$

with the partial quadratic loss function associated with the $i$th gyro

$$J_i(u_i) = \lim_{n\to\infty} \frac{1}{n} E\left\{ \sum_{k=0}^{n} |\beta_i(k)|^2 + q^2 |u_i(k)|^2 \right\} \tag{30}$$

The optimal control has the form

$$\omega_c(k) = U\tilde{\Omega}(k) - \begin{pmatrix} L_1 x_1(k) \\ L_2 x_2(k) \\ L_3 x_3(k) \end{pmatrix} \tag{31}$$

where $L_i$ are the steady-state optimal feedback gains computed off line given the solution of the usual Riccati equations:

$$S_i = F_i^t S_i F_i - F_i^t S_i G_i (G_i^t S_i G_i + q^2 I_2)^{-1} \times G_i^t S_i F_i + H_i^t H_i \tag{32}$$

$$L_i = F_i^t S_i G_i [G_i^t S_i G_i + q^2 I_2)]^{-1} \tag{33}$$

By using the separation theorem of LQG control theory,[6] we have, in the stochastic case

$$\omega_c(k) = U\hat{\tilde{\Omega}}(k) - \begin{pmatrix} L_1 \hat{x}_1(k) \\ L_2 \hat{x}_2(k) \\ L_3 \hat{x}_3(k) \end{pmatrix} = -L\hat{x}(k) \tag{34}$$

where the estimates are given by Eq. (23). A block diagram of the system is shown in Fig. 3.

*Remarks*

1) In the actual design, $y$ is the output of a notch filter with frequencies $N$, $2N$, $3N$, . . . in order to suppress periodic noise on the $\beta_i$ pickoff outputs.

2) It can also be shown that the regulator has an integral action because of the model (20) chosen for $\tilde{\Omega}$.

3) In the actual design, static error models for the sensors, including DTG biases and misalignment, have been taken into account in the three DTG models to improve accuracy.[7]

## Performance Results

### Estimator Performances

A 2000-Hz sampling frequency $fs$ was selected for the 6 input/6 output system. Figure 4 shows the estimator frequency response for the $X$ axis. The responses of other axes are similar. The unity steady-state gain is verified. The gap between measurements and simulation is mainly due to

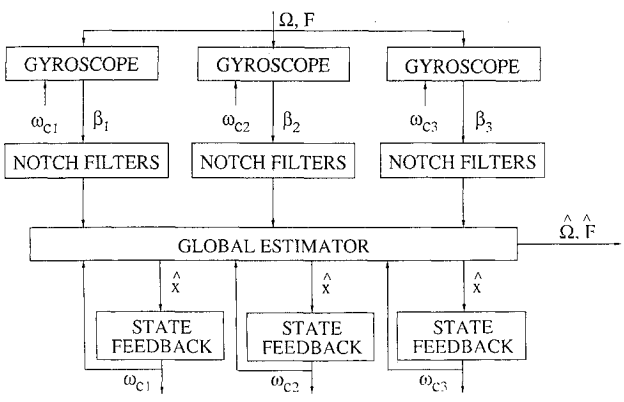


**Fig. 3 LQG control of three unbalanced gyroscopes.**

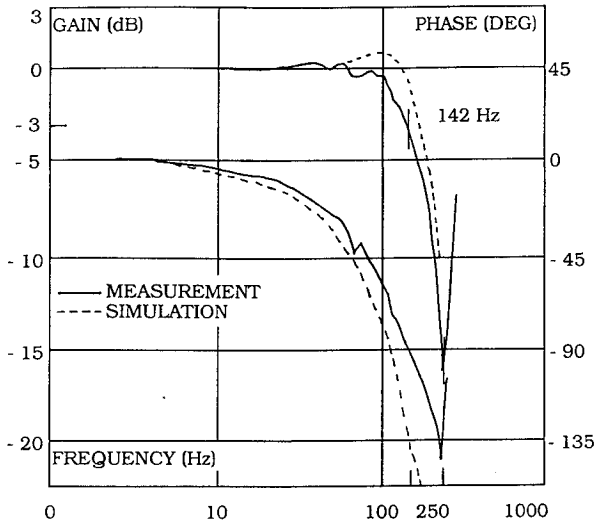


**Fig. 4 Bode plot for the estimator transfer function $\hat{\Omega}_X/\Omega_X$.**

turntable resonances above 60 Hz. The effect of the notch filters at 250 Hz can be seen: the bandwidth cannot be greater than the spin frequency. A 140-Hz bandwidth with less than 1 dB resonance is shown: more than half of the spin frequency is achieved. This is twice the bandwidth of conventional implementations where the estimation $\hat{\omega}$ is taken to be $\omega_c$, thus limiting the bandwidth of the estimator to that of the control loop. In the proposed method, these two bandwidths are distinct: stabilization error is used to improve the estimation. Day-to-day drift is 10 deg/h and bias error is 3 mg with a measurement range of 1000 deg/s and 100 g.

#### Feedback Performances

Feedback properties of the proposed design, e.g., disturbance rejection, stability margins, and sensitivity to model errors, are now analyzed using multivariable techniques. These properties are related to the Bode magnitude vs frequency plots of the maximum singular values of the sensitivity matrix $S$ and of the closed-loop transfer matrix $T$. (The inverse of $S$ is also called the return difference matrix.) The state-space representation of Eqs. (21), (23), and (34) is equivalent to the following input-output representation:

Plant:

$$\begin{cases} \beta = M\omega_c + d \\ \text{with } M = H(zI_{18} - F)^{-1}G\omega_c \end{cases} \tag{35}$$

Controller:

$$\begin{cases} \omega_c = \Gamma(\beta_R - y) \\ \text{with } \Gamma = L(zI_{18} - F + GL + KH)^{-1}K \end{cases} \tag{36}$$

Disturbance model:

$$d = H(zI_{18} - F)^{-1}\nu \tag{37}$$

Sensors:

$$y = \beta + w \tag{38}$$

where $\beta_R$ is the reference input; zero in the present case. This leads to the closed-loop representation:

$$\beta = T(\beta_R - w) + Sd \tag{39}$$

with

$$\begin{cases} T = (I_6 + M\Gamma)^{-1}M\Gamma \\ S = (I_6 + M\Gamma)^{-1} \end{cases} \tag{40}$$

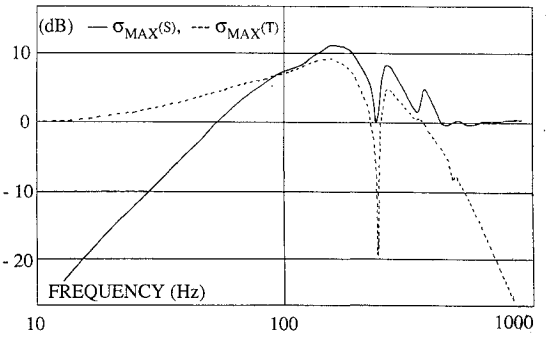


**Fig. 5 Bode plots for $\sigma_{max}(S)$ and $\sigma_{max}(T)$.**

Quantitative measures of feedback properties are now given by the following[8]:

Disturbance and noise attenuation:

$$\max_{d \neq 0,\ w = 0} \frac{\|\beta\|}{\|d\|} = \sigma_{max}(S) \tag{41}$$

$$\max_{d = 0,\ w \neq 0} \frac{\|\beta\|}{\|w\|} = \sigma_{max}(T) \tag{42}$$

Stability margin:

$S$ and $T$ are stable as soon as $\forall\omega$, with $z = e^{j\omega/fs}$

$$\sigma_{max}[\Delta(M\Gamma)(z)] < \frac{1}{\sigma_{max}[T(z)]} \tag{43}$$

where the true value of $M'\Gamma'$ is related to the nominal value $M\Gamma$ by

$$M'\Gamma' = [I_6 + \Delta(M\Gamma)]M\Gamma \tag{44}$$

Plant output sensitivity to plant variations:

$$\sigma_{max}(\Delta T) \leq \sigma_{max}(S) \cdot \sigma_{max}(\Delta M) \tag{45}$$

with

$$\begin{cases} M' = (I_6 + \Delta M)^{-1}M \\ T' = (I_6 + \Delta T)^{-1}T \end{cases} \tag{46}$$

The Bode plots for $\sigma_{max}(S)$ and $\sigma_{max}(T)$ are given in Fig. 5. The $S$ plot shows that constant disturbances are exactly rejected, and noise under 50 Hz is attenuated by an equivalent high-pass second-order filter. The $T$ plot shows that the worst stability margin occurs at 160 Hz where the model is still of good quality, so that Eq. (43) is satisfied. The stability margin above 500 Hz is better than 6 dB. The 250-Hz sensor noise (part of $w$) is strongly rejected by the notch filters.

Experiments show that the stiffness is three times greater than in the case of classical control and the sensor can stand angular acceleration up to 60,000 deg/s$^2$. This is made possible because the control loop can be tuned, by choosing $q$, without detuning the estimator. This last tuning is obtained by choosing the covariance matrix of the noises $\nu_\Omega$.

## Conclusions

The principle of a six-axis forced-balance sensor to measure angular rate and acceleration is presented. This principle involves using three dry tuned gyroscopes, two of which are unbalanced. It is an alternative for inertial measurement units based on two gyroscopes and three accelerometers. This leads to savings in space, weight, and cost.

The bandwidth of this forced-balance sensor is improved by using the outputs of detectors, a model taking into account the coupled high-frequency dynamics and a linear quadratic Gaussian estimator/controller. Details of the implementation

along with performances are presented. The resulting angular rate bandwidth is greater than half of the spin frequency.

Compared with classical inertial measurement units, acceleration precision is competitive and acceleration bandwidth is smaller (half of the spin frequency). The whole performances are nevertheless sufficient for guidance of agile missiles.

## Acknowledgments

The authors would like to thank L. Camberlein and C. Leclercq for many helpful discussions. Help from J. M. Noël is highly appreciated.

## References

[1]Steel, G. K., and Puri, S. N. "Direct Digital Control of Dry Tuned Rotor Gyros," *Automatic Control in Space,* Vol. 2, Pergamon, Oxford, England, UK, 1980, pp. 79–85.

[2]Riberio, J. F., "A LQG Regulator for the Angular Motion of the Rotor of a Tuned Gyroscope," Instituto de Pesquisas Espaciais, INPE-4280, PRE/1152, Sao José dos Campos, Brazil, Aug. 1987.

[3]Craig, R. J. G., "Theory of Operation of an Elastically Supported Tuned Gyroscope," *IEEE Transactions on Aerospace and Electronic Systems,* Vol. AES 2, No. 3, May 1972, pp. 280–288.

[4]Craig, R. J. G., "Dynamically Tuned Gyros in Strapdown Systems," NATO-AGARD *Inertial Navigation, Components, and Systems,* AD-758127, CP116, Paris, 1973, pp. 12.1–12.A1.9.

[5]Constancis, P., and Sorine, M., "Wideband Linear Quadratic Gaussian Control of Strapdown Dry Tuned Gyro/Accelerometers," *Proceedings of the AIAA Guidance, Navigation and Control Conference,* AIAA, Washington, DC, 1989, pp. 141–145; AIAA Paper 89-3441, Aug. 1989.

[6]Aström, K. J., and Wittenmark, B., *Computer-Controlled Systems: Theory and Design,* Prentice-Hall, Englewood Cliffs, NJ, 1984, pp. 254–281.

[7]Constancis, P., "Modélisation et Commande des Gyroscopes Secs Accordés d'une Centrale Inertielle à Composants Liés," Ph.D. Thesis, University of Paris IX, Dauphine, March 1990.

[8]Safanov, M. G., Laub, A. J., and Hartmann, G. L., "Feedback Properties of Multivariable Systems: The Role and Use of the Return Difference Matrix," *IEEE Transactions on Automatic Control,* Vol. AC-26, No. 1, Feb. 1981, pp. 47–65.

[9]Bellman, R., *Introduction to Matrix Analysis,* McGraw-Hill, New York, 1960.